J. Astrophys. Astr. (2020) 41:46
https://doi.org/10.1007/s12036-020-09673-4

Carbon-enhanced metal-poor stars enriched in s-process and r-process elements

DRISYA KARINKUZHI[1,2,*], SOPHIE VAN ECK[2], ALAIN JORISSEN[2], STEPHANE GORIELY[2], LIONEL SIESS[2], THIBAULT MERLE[2] and THOMAS MASSERON[3,4]

[1]Department of Physics, Indian Institute of Science, Bengaluru 560012, India.
[2]Institut d'Astronomie et d'Astrophysique, Université Libre de Bruxelles, ULB, Campus Plaine C.P. 226, Boulevard du Triomphe, B-1050 Brussels, Belgium.
[3]Instituto de Astrofísica de Canarias, 38205 La Laguna, Tenerife, Spain.
[4]Departamento de Astrofísica, Universidad de La Laguna, 38206 La Laguna, Tenerife, Spain.
Corresponding author. E-mail: drisyadev@gmail.com

MS received 1 September 2020; accepted 28 September 2020; published online 17 December 2020

Abstract. We present an on-going project consisting of analysis of a sample of twenty-five metal-poor stars, most of them carbon-enriched and thus tagged carbon-enhanced metal-poor (CEMP) stars, observed with the high-resolution HERMES spectrograph mounted on the Mercator telescope (La Palma), the UVES spectrograph on VLT (ESO Chile), or the HIRES spectrograph on KECK (Hawaii). This sample consists of CEMP-s stars, which are CEMP stars enriched in slow-neutron-capture (s-process) elements, as well as CEMP-rs stars enriched with both s-process and rapid-neutron-capture (r-process) elements. We also included an r-process-enriched star for comparison purposes. The origin of the abundance differences between CEMP-s and CEMP-rs stars is presently unknown. It has been claimed that the i-process (intermediate nucleosynthesis process), whose site still remains to be identified, could better reproduce CEMP-rs abundances than the s-process. We aim at understanding whether the i-process and its putative site can reproduce the abundance pattern measured in CEMP-rs stars.

Keywords. Stars: abundances—stars: AGB and post-AGB—binaries: spectroscopic—stars: fundamental parameters.

1. Introduction

Elements heavier than iron are mainly produced by two neutron-capture processes, called slow-neutron-capture process (s-process) and rapid-neutron-capture process (r-process), and result from the competition between neutron captures and β-decay timescales. These two processes require different astrophysical conditions (different neutron densities and temperatures); hence the astrophysical sites at which they occur must be distinct. While low-mass to intermediate-mass asymptotic-giant-branch (AGB) stars are firmly identified as the site for the s-process, the r-process site is still debated, though recent studies (Abbott *et al*. 2017; Drout *et al*. 2017) revived neutron-star mergers as a very plausible r-process site (Goriely *et al*. 2011; Thielemann *et al*. 2017). From the observational point of view, stars enriched in s-process elements have been identified both at high metallicities ($-1 \leq$ [Fe/H] ≤ 0, CH, barium and S stars) and, among carbon-enhanced metal-poor (CEMP) stars, at lower metallicities ($-3.0 \leq$ [Fe/H] ≤ -1.0). As far as r-process-enriched stars are concerned, they are generally found among lower-metallicity stars ([Fe/H] ≤ -2.0). On top of these two categories, among CEMP stars a few stars were

This article is part of the Topical Collection: Chemical elements in the Universe: Origin and evolution.

identified with a hybrid enrichment of both s-process and r-process elements and hence named CEMP-rs stars. The origin of the peculiar abundances in CEMP-rs stars, whose binarity is not yet confirmed, is still an open question. There were many attempts to interpret the observed abundances in these stars using a superposition of s-process and r-process elements successively produced in two independent sites (Cohen *et al*. 2003; Zijlstra 2004; Wanajo *et al*. 2006; Bisterzo *et al*. 2011). As noted by Lugaro *et al*. (2012) and Abate *et al*. (2016) this scenario is difficult to reconcile with both the CEMP-rs statistics and their high [hs/ls] ratios (ratio of heavy s-process elements to light s-process elements). This tension prompts to look for a single astrophysical site that could produce both r-process and s-process elements at levels compatible with those measured in CEMP-rs stars. An intermediate nucleosynthesis process (i-process) originally proposed by Cowan & Rose (1977), occurring at a neutron density $N_n \sim 10^{15}$ cm^{-3}, intermediate between that of the s-process ($N_n \sim 10^8$ cm^{-3}) and that required by the r-process ($N_n > > 10^{20}$ cm^{-3}), is another possible scenario to explain the hybrid r-process and s-process enrichment in CEMP-rs stars. While i-process simulations tend to reproduce the abundances in CEMP-rs stars convincingly (Hampel *et al*. 2016), the astrophysical site of such a process remains to be identified.

The aim of the present on-going investigation is to compare the CEMP-s and CEMP-rs star-abundance ratios to check whether these ratios show some kind of continuity from CEMP-s to CEMP-rs stars, or whether instead we can define two very different abundance groups, which would tend to indicate that the process (and maybe the site) producing CEMP-rs stars would be drastically different from the one producing CEMP-s objects.

2. Data and observation

High-resolution spectra for most of the objects have been acquired (resolution $R \sim 86\,000$) with the HERMES spectrograph (Raskin *et al.* 2011) mounted on the 1.2 m Mercator telescope at the Roque de los Muchachos Observatory, La Palma, Canary Islands, which covers the wavelength range 3900–9000 Å. These objects are observed as part of a long-term monitoring of radial velocities to detect the binary nature and derive orbital parameters of specific families of stars (Gorlova *et al*. 2014). Spectra recorded on different nights were co-added after correcting for the Doppler shifts to maximize signal-to-noise ratio (SNR). We also used a few spectra obtained with the UVES spectrograph mounted on the ESO *Very Large Telescope* with a wavelength coverage from 3300 to 6800 Å. Spectra of three stars were taken from the HIRES/KECK data archive and have wavelength coverage from 3700 to 8000 Å.

3. Derivation of atmospheric parameters and abundances

Atmospheric parameters of the program stars were derived using the BACCHUS pipeline (Masseron *et al*. 2016) in semi-automated mode. BACCHUS uses the 1D local thermodynamical equilibrium (LTE) spectrum-synthesis code TURBOSPECTRUM (Alvarez & Plez 1998; Plez 2012). We started the iteration with the photometric estimates derived using Alonso *et al*. (1996, 1999) calibrations. We also performed the spectral fitting of the C_2 band at 5165 Å and of the CN region around 6500 Å to get an initial estimate of the C and N abundances so as to derive the equivalent widths of Fe lines by taking care of the possible blends caused by these molecules. To check the quality of the spectral fit with the adopted atmospheric parameters, we used the KASTEEL code, which relies on a spectral-fitting method of selected wavelength ranges sensitive to the atmospheric parameters. We used eight wavelength ranges; namely the region around the Ca II H&K lines at 3933 and 3968 Å, the CH band in the range [3985–4050] Å, the region around the CN line at 4215 Å and the Ca I line at 4226 Å, $^{12}C^{12}C$ and $^{13}C^{12}C$ bands in the region [4725–4755] Å, the region of H_β [4830–4890] Å, the C_2 Swan band and the Mg I b triplet in the region [5150–5190] Å, the region around the [OI] line at 6300 Å, and the region of H_α including the Ba II line at 6496.9 Å [6490–6600] Å. We present the derived atmospheric parameters along with the information about the possible binary nature of the sample stars in Table 1.

Abundances were then derived by comparing observed and synthetic spectra generated with the TURBOSPECTRUM radiative-transfer code using the MARCS model atmospheres corresponding to the derived stellar parameters and under the assumption of local thermodynamic equilibrium (LTE). Non-LTE (NLTE) corrections (from various sources: Asplund *et al*. 2005; Mashonkina *et al*. 2008, 2012; Amarsi *et al*. 2016) were applied when available for the elements O, Eu and Pb. We also included hyperfine (HF) splitting for the atomic lines and used carbon-enriched MARCS models when available. Solar abundances

Table 1. Program stars and adopted atmospheric parameters (ξ is the microturbulent velocity). The column labeled Spec refers to the spectrograph used (U, H and HI correspond to UVES, HERMES and HIRES, respectively), the Class column refers to the star assignment based on the [La/Eu] ratio (Section 4), and Bin refers to binarity as reported in the reference indicated in the Ref. column; '?' indicates 'possible spectroscopic binary'

Name	$T_{\rm eff}$ (K)	$\log g$ (cgs)	ξ (km s^{-1})	[Fe/H]	[La/Fe]	[Eu/Fe]	Class	Spec	Bin	Ref.
CS 22887-048	6500 ± 50	3.20 ± 0.15	1.00 ± 0.05	−2.10 ± 0.09	1.90	1.33	s	U	–	-
CS 22891-171	5215 ± 68	1.24 ± 0.09	2.14 ± 0.14	−2.50 ± 0.10	2.25	1.73	rs	U	–	-
CS 22942-019	5100 ± 98	2.19 ± 0.20	1.73 ± 0.10	−2.50 ± 0.09	1.34	0.78	s	U	Y	d,g
CS 30322-023	4500 ± 100	1.00 ± 0.50	2.80 ± 0.10	−3.35 ± 0.09	1.05	0.23	s	U	–	-
HD 26	5169 ± 108	2.46 ± 0.18	1.46 ± 0.08	−0.98 ± 0.09	1.78	0.86	s	H	Y	b
HD 5223	4650 ± 120	1.03 ± 0.30	2.16 ± 0.14	−2.00 ± 0.08	1.46	1.18	rs	H	Y	e
HD 55496	4642 ± 39	1.65 ± 0.14	1.33 ± 0.08	−2.10 ± 0.09	0.83	-	s	H	Y?	g
HD 76396	4750 ± 100	2.00 ± 0.30	2.00 ± 0.10	−2.27 ± 0.10	1.87	1.65	rs	H	Y	b
HD 145777	4443 ± 57	0.50 ± 0.10	2.63 ± 0.10	−2.32 ± 0.10	1.07	0.97	rs	H	Y	b,c
HD 187861	5000 ± 100	1.50 ± 0.25	2.00 ± 0.20	−2.60 ± 0.10	1.81	1.88	rs	U	–	-
HD 196944	5168 ± 48	1.28 ± 0.16	1.68 ± 0.11	−2.50 ± 0.09	0.77	0.79	rs	H	Y	a
HD 198269	4458 ± 15	0.83 ± 0.08	1.64 ± 0.09	−2.10 ± 0.10	1.22	0.67	s	H	Y	e
HD 201626	5084 ± 77	2.18 ± 0.16	1.60 ± 0.09	−1.75 ± 0.10	1.65	0.78	s	H	Y	e
HD 206983	4200 ± 100	0.60 ± 0.20	1.50 ± 0.10	−1.00 ± 0.10	0.75	0.45	rs	H	Y?	g
HD 209621	4740 ± 55	1.75 ± 0.25	1.94 ± 0.13	−2.00 ± 0.09	1.90	1.78	rs	H	Y	e
HD 221170	4577 ± 50	0.77 ± 0.20	1.84 ± 0.10	−2.40 ± 0.10	0.45	0.53	r	H	N	h
HD 224959	4969 ± 64	1.26 ± 0.29	1.63 ± 0.14	−2.36 ± 0.09	2.16	1.99	rs	H	Y	e
HE 0111-1346	4687 ± 102	1.26 ± 0.30	1.77 ± 0.16	−2.10 ± 0.09	1.91	1.38	s	H	Y	b,f
HE 0151-0341	4820 ± 112	1.15 ± 0.08	1.72 ± 0.16	−2.89 ± 0.08	1.84	1.67	rs	HI	Y	f
HE 0319-0215	4738 ± 100	0.66 ± 0.40	2.16 ± 0.10	−2.90 ± 0.10	1.70	1.31	rs	HI	Y	f
HE 0507-1653	5035 ± 53	2.39 ± 0.16	1.53 ± 0.14	−1.35 ± 0.10	1.78	1.13	s	H	Y	b,f
HE 1120-2122	4500 ± 100	0.50 ± 0.50	1.50 ± 0.10	−2.00 ± 0.10	1.33	1.33	rs	H	Y	b,c
HE 1429-0551	4832 ± 41	1.14 ± 0.20	2.01 ± 0.14	−2.70 ± 0.10	1.30	1.08	rs	H	N	b,c
HE 2144-1832	4250 ± 100	0.50 ± 0.30	2.00 ± 0.15	−1.85 ± 0.10	1.68	1.28	rs	H	Y?	b,c
HE 2255-1724	4776 ± 51	1.64 ± 0.15	1.84 ± 0.15	−2.32 ± 0.09	1.61	1.07	rs	HI	–	-

References for Bin column: (a) HERMES unpublished data, (b) Jorissen *et al.* (2016), (c) Jorissen *et al.* (in prep.), (d) Preston & Sneden (2001), (e) McClure & Woodsworth (1990), (f) Hansen *et al.* (2016), (g) Jorissen *et al.* (2005), (h) Hansen *et al.* (2015)

were taken from Asplund *et al.* (2009). This way, we aimed at deriving the abundances of light elements C, N, O, Na, Mg, Ca, Sc, Ti, Cr, Mn, Co, Ni, Cu, Zn as well as light s-process elements (Sr, Y, Zr), heavy s-process elements (Ba, La, Ce, Pr, Nd), very heavy s-process elements (Pb), and r-process elements (Sm, Eu, Gd, Dy, Er, Hf, Os).

4. CEMP object classification

The classification of CEMP stars into CEMP-s and CEMP-rs is generally based on their Ba/Eu or La/Eu abundance ratios. We adopted a classification scheme similar to the one proposed by Beers & Christlieb (2005) but based on lanthanum instead of barium. These two elements are neighbours in the periodic table but lanthanum lines are more numerous and weaker. Therefore, they should in principle provide more reliable abundances. Our new classification based on lanthanum gives:

- CEMP-s: [La/Fe] $> +1$ and [La/Eu] $> +0.5$
- CEMP-rs: $0.0 <$ [La/Eu] $< +0.5$
- CEMP-rI: [La/Eu] < 0, $0 <$ [Eu/Fe] $< +1$
- CEMP-rII: [La/Eu] < 0, [Eu/Fe] $> +1$

If the abundances of Ba, La or Eu are not available, then the objects cannot be easily classified. Also, r-process abundances are scarce in the literature. In most cases, these stars are included in the CEMP-s group based on the enrichment of s-process elements, without considering whether this enrichment is merely a consequence of a strong r-process enrichment. The case of the well-known CH star HD 5223 is a good example of this difficulty. Since the abundance of europium or of any other r-process element is not

available for this object, it was considered as a CEMP-s star until now. In the present paper, we derive [Ba/Eu] = 0.24 and [La/Eu] = 0.28 for this object, making it a definite CEMP-rs object.

Two objects are found to be border cases, namely CS 22891-171 ([La/Eu] = 0.52) and HE 2255-1754 ([La/Eu] = 0.54). We considered them as CEMP-rs stars. After re-assignment, fifteen of our program stars can be assigned to the CEMP-rs class and nine of them belong to the CEMP-s group.

Figure 1 presents the objects in the ([La/Fe], [Eu/Fe]) plane together with CEMP-s, CEMP-rs and r-process-enriched stars from the literature.

The overlap of our CEMP-s stars with CEMP-s stars collected from the literature is very good, though our stars extend to larger s-process enrichments, especially CS 22887-048 and HE 0111-1346 at [La/Fe] ≈ 2. Most of these CEMP-s objects fall however slightly below s-process predictions for a 1.5 $M_\odot$ star of [Fe/H] $= -1$ (5^{th} thermal pulse).

The [La/Fe] ratios of CEMP-rs stars encompass those of CEMP-s stars, but they are located at higher

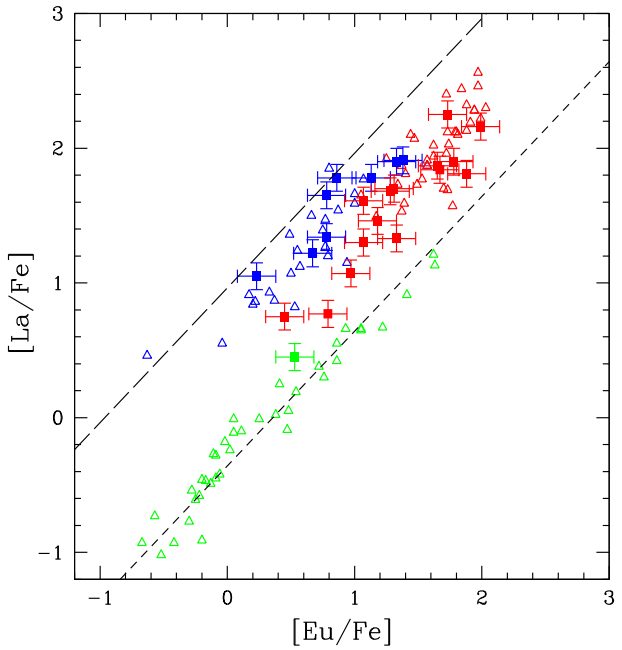

Figure 1. Abundances of [La/Fe] *vs* [Eu/Fe]. Target CEMP-s, CEMP-rs and r-process-enriched stars for this study are represented by blue, red and green squares respectively. The blue, red and green triangles are CEMP-s, CEMP-rs and r-process-enriched stars (includes both CEMP-r and r-process stars without carbon enrichment) from the literature. The short-dash line corresponds to abundance ratio scaling with a pure solar r-process (Goriely 1999), whereas the long-dash line corresponds to s-process nucleosynthesis abundance ratio scaling with the predictions for a 1.5 $M_\odot$ star of [Fe/H] $= -1$ (5^{th} pulse)

[Eu/Fe] ratio for a similar [La/Eu] enrichment. While the literature CEMP-rs stars are restricted to very large [La/Fe] and [Eu/Fe] enrichments (larger than 1.5 and 1 dex, respectively), our sample of CEMP-rs stars extends to lower [La/Fe] and [Eu/Fe] ratios (Figure 1). A reason is that europium abundances were not systematically determined in CEMP-s objects, which could then not be classified as CEMP-rs. Also, it seems that europium was determined only in the most enriched CEMP-s stars, while in our study we now systematically undertake its determination even in objects with a lower enrichment level.

The two CEMP-rs objects with the lowest [La/Fe] and [Eu/Fe] abundances are HD 196944 and HD 206983. Their overall heavy-element enrichment is low compared to other CEMP-rs stars. For HD 206983, [C/Fe] ratio is also mild and amounts to 0.42 dex. Masseron *et al.* (2010) classified HD 196944 as CEMP-s and HD 206983 as a 'low-s' star.

Another striking result is the continuity observed between CEMP-s and CEMP-rs stars. While it is easier to distinguish CEMP-r objects, drawing a line between CEMP-s and CEMP-rs stars turns out to be somewhat artificial, which explains that several objects are actually border cases that could well be assigned to either category.

5. Discussion

The intermediate neutron densities required for the operation of the i-process ($N_n \approx 10^{15}$ cm^{-3}) can be produced by the operation of $^{22}\text{Ne}(\alpha, n)^{25}\text{Mg}$ in the hot thermal pulses of intermediate-mass AGB stars (Goriely & Siess 2005). Alternatively, the ingestion of protons in a He-burning convective region could trigger an i-process, as first described by Cowan & Rose (1977). Among the different sites that have been proposed for this i-process, we mention (i) proton ingestion in very-metal-poor low-mass stars during the core He-flash or at the beginning of the TP-AGB phase, (ii) the dredge-out in super-AGB stars, (iii) the late pulses in post-AGB stars, and (iv) He-shell flashes in rapidly accreting white dwarfs (see Karakas & Lattanzio 2014; Denissenkov *et al.* 2017, and references therein). Finally, three-dimensional simulations show that turbulence could trigger proton ingestion episodes at metallicities close to solar during the core He-flash (Mocák *et al.* 2008; 2009; 2010) in stars of masses M ≤ 2.25 $M_\odot$.

Constraining the mass of stars responsible for the CEMP-rs abundance pattern could thus give important clues to the physical conditions at work in the i-process.

Table 1 reveals the high binarity incidence among CEMP-rs objects: they consist of 60 to 73% binaries, compared to 66 to 77% for CEMP-s stars. The only RV-constant CEMP-rs star of our sample is HE 1429-0551, with $\sigma_{RV} = 0.186$ km s^{-1} after about nine years of monitoring (Karinkuzhi *et al.* 2020). The other non-binary star of our sample is HD 221170, which is an r-process-enriched star. This is not unusual since Hansen *et al.* (2016) found a normal binary frequency of $19\% \pm 6\%$ in a CEMP-r sample. Like CEMP-s stars, CEMP-rs objects thus appear to be extrinsic objects that have been polluted by a companion in the past. Unfortunately the mass of the polluting star is not well constrained, apart from the fact that it should be more massive than the current CEMP star. However, well-chosen abundance ratios showing a mass dependence could provide some hint. Detailed abundance profiles are under study and will be published in Karinkuzhi *et al.* (2020).

Acknowledgements

D.K. acknowledges the financial support from Science and Engineering Research Board (SERB), DST, India, through the file number PDF/2017/002338; CSIR, India, through the file No.13(9086-A)2019-Pool; and FNRS, Belgium, through visiting research fellowship. S.V.E. thanks the Fondation ULB for its support. L.S. and S.G. are senior FNRS research associates. T.Me. is supported by a grant from the Fondation ULB. T.Ma. acknowledges support by the MINECO under grant AYA-2017-88254-P.

References

Abate C., Stancliffe R. J., Liu. Z.-W. 2016, A&A, 587, A50
Abbott B. P., Abbott R., Abbott T. D. *et al.* 2017, ApJ, 848L, 13
Alonso A., Arribas S., Martinez-Roger C. 1996, A&AS, 117, 227
Alonso A., Arribas S., Martínez-Roger C. 1999, A&AS, 139, 335
Alvarez R., Plez B. 1998, A&A, 330, 1109
Amarsi A. M., Asplund M., Collet R., Leenaarts J. 2016, MNRAS, 455, 3735
Asplund M., Grevesse N., Sauval A. J. *et al.* 2005, A&A, 435, 339
Asplund M., Grevesse N., Sauval A. J., Scott P. 2009, ARA&A, 47, 481
Beers T. C., Christlieb N. 2005, ARA&A, 43, 531
Bisterzo S., Gallino R., Straniero O., Cristallo S., Käppeler F. 2011, MNRAS, 418, 284
Cohen J. G., Christlieb N., Qian Y.-Z., Wasserburg G. J. 2003, ApJ, 588, 1082
Cowan J. J., Rose W. K. 1977, ApJ, 212, 149
Denissenkov P. A., Herwig F., Battino U. *et al.* 2017, ApJ, 834, L10
Drout M. R., Piro A. L., Shappee B. J., Kilpatrick C. D. *et al.* 2017, Science, 358, 1570
Goriely S. 1999, A&A, 342, 881
Goriely S., Siess L. 2005, in IAU Symposium, Vol. 228, From Lithium to Uranium: Elemental Tracers of Early Cosmic Evolution, ed. V. Hill, P. Francois, & F. Primas, 451–460
Goriely S., Bauswein A., Janka H. T. 2011, ApJ, 738L, 32
Gorlova N., Van Winckel H., Vos J. *et al.* 2014, arXiv e-prints, arXiv:1403.2287
Hampel M., Stancliffe R. J., Lugaro M., Meyer B. S. 2016, ApJ, 831, 171
Hansen T. T., Andersen J., Nordström B. *et al.* 2015, A&A, 583, A49
Hansen T. T., Andersen J., Nordström B. *et al.* 2016, A&A, 588, A3
Jorissen A., Zacs L., Udry S., Lindgren H., Musaev F. A., 2005, A&A, 441,1135
Jorissen A., Van Eck S., Van Winckel H. *et al.* 2016, A&A, 586, A158
Karakas Amanda I., Lattanzio John C., 2014, PASA, 31, 30
Karinkuzhi D., Van Eck S., Goriely S. *et al.* A&A, arxiv: 2010.13620
Lugaro M., Karakas A. I., Stancliffe R. J., Rijs C. 2012, ApJ, 747, 2
Mashonkina L., Zhao G., Gehren T. *et al.* 2008, A&A, 478, 529
Mashonkina L., Ryabtsev A., Frebel A. 2012, A&A, 540, A98
Masseron T., Johnson J. A., Plez B. *et al.* 2010, A&A, 509, A9
Masseron T., Merle T., Hawkins K. 2016, BACCHUS: Brussels Automatic Code for Characterizing High accUracy Spectra, Astrophysics Source CodeLibrary, 1605.004
McClure R. D., Woodsworth A. W. 1990, ApJ, 352, 709
Mocák M., Müller E., Weiss A., Kifonidis K. 2008, A&A, 490, 265
Mocák M., Müller E., Weiss A., Kifonidis K. 2009, A&A, 501, 659
Mocák M., Campbell S. W., Müller E., Kifonidis K. 2010, A&A, 520, 114
Plez B. 2012, Turbospectrum: Code for spectral synthesis, Astrophysics Source Code Library, 1205.004
Preston G. W., Sneden C. 2001, AJ, 122, 1545
Thielemann F.-K., Eichler M., Panov I. V., Wehmeyer B. 2017, ARNPS 67, 253
Wanajo S., Nomoto K., Iwamoto N., Ishimaru Y., Beers T. C. 2006, ApJ, 636, 842
Zijlstra A. A. 2004, MNRAS, 348, L23